Preparation, characterization and comparison of antibacterial property of polyethersulfone...

Article · January 2017

DOI: 10.12989/mwt.2017.8.1.051

CITATIONS
0

READS
62

8 authors, including:

Nadir Dizge
Gebze Technical University
47 PUBLICATIONS **1,239** CITATIONS
SEE PROFILE

Utku Bulut Simsek
Mersin University
10 PUBLICATIONS **0** CITATIONS
SEE PROFILE

Meral Turabik
Mersin University
19 PUBLICATIONS **485** CITATIONS
SEE PROFILE

Kasim Ocakoglu
Mersin University
66 PUBLICATIONS **625** CITATIONS
SEE PROFILE

Membrane Water Treatment, *Vol. 8, No. 1 (2017) 51-71*
DOI: https://doi.org/10.12989/mwt.2017.8.1.051

Preparation, characterization and comparison of antibacterial property of polyethersulfone composite membrane containing zerovalent iron or magnetite nanoparticles

Nadir Dizge*[1], Yasin Ozay[1], U. Bulut Simsek[2], H. Elif Gulsen[1], Ceyhun Akarsu[1], Meral Turabik[2,3], Ali Unyayar[1] and Kasim Ocakoglu[4]

[1]*Department of Environmental Engineering, Mersin University, 33343 Yenisehir, Mersin, Turkey*
[2]*Department of Nanotechnology and Advanced Materials, Mersin University, 33343 Yenisehir, Mersin, Turkey*
[3]*Department of Chemical Programme Technical Science Vocational School, Mersin University, 33343 Yenisehir, Mersin, Turkey.*
[4]*Department of Energy Systems Engineering, Mersin University, 33480 Mersin, Turkey*

(*Received April 11, 2016, Revised October 13, 2016, Accepted October 15, 2016*)

Abstract. Antimicrobial polyethersulfone ultrafiltration membranes containing zerovalent iron (Fe^0) and magnetite (Fe_3O_4) nanoparticles were synthesized via phase inversion method using polyethersulfone (PES) as membrane material and nano-iron as nanoparticle materials. Zerovalent iron nanoparticles (nZVI) were prepared by the reduction of iron ions with borohydride applying an inert atmosphere by using N_2 gases. The magnetite nanoparticles (nMag) were prepared via co-precipitation method by adding a base to an aqueous mixture of Fe^{3+} and Fe^{2+} salts. The synthesized nanoparticles were characterized by scanning electron microscopy, X-ray powder diffraction, and dynamic light scattering analysis. Moreover, the properties of the synthesized membranes were characterized by scanning electron microscopy energy dispersive X-ray spectroscopy and atomic force microscopy. The PES membranes containing the nZVI or nMag were examined for antimicrobial characteristics. Moreover, amount of iron run away from the PES composite membranes during the dead-end filtration were tested. The results showed that the permeation flux of the composite membranes was higher than the pristine PES membrane. The membranes containing nano-iron showed good antibacterial activity against gram-negative bacteria (*Escherichia coli*). The composite membranes can be successfully used for the domestic wastewater filtration to reduce membrane biofouling.

Keywords: zerovalent iron nanoparticles; magnetite nanoparticles; polyethersulfone membrane; phase inversion; antimicrobial membrane

1. Introduction

Nanotechnology is a thriving working area that includes a wide range of technologies which are under development in nanoscale. It plays a huge role in the progress of innovative methods to produce new products, to formulate new materials and chemicals (Mansoori, Bastami *et al*. 2008). Nanoparticles are one of the new scientific research fields of nanotechnology due to potential

*Corresponding author, Professor, E-mail: nadirdizge@gmail.com

 ISSN: 2005-8624 (Print), 2092-7037 (Online)

applications in biomedical, optical, chemical, environmental, electronic fields and etc. (Abhilash 2010, Nikalje 2015, Lefevre, Bossa *et al*. 2016).

Magnetic nanoparticles are classified as nanoparticle materials of smaller then 100 nm. They are generally formed such magnetic elements of iron, cobalt, chrome and their chemical compounds like magnetite (Fe_3O_4), maghemite (Fe_2O_3), cobalt ferrite (Fe_2CoO_4), chromium dioxide (Cr_2O) (Yang, Liu *et al*. 2008). Several methods perform for preparing magnetic nanoparticle such as co-precipitation (Ayyappan, Philip *et al*. 2009), thermal decomposition (Hufschmid, Arami *et al*. 2015), micro-emulsion (Chen, Kong *et al*. 2015) and flame spray synthesis (Grass, Athanassiou *et al*. 2007). An extensive diversity of applications has been determined for magnetic nanoparticles which include medical diagnostics and treatments (Rosenberger, Strauss *et al*. 2015), magnetic immunoassay (Sumin and Lim 2015), wastewater treatment (Yu, Hao *et al*. 2015), drinking water treatment (Simeonidis, Kaprar *et al*. 2015), chemistry (Iniyavan, Balaji *et al*. 2015), biomedical imaging (Colombo, Carregal-Romero *et al*. 2012) and genetic engineering (Cheng, Huang *et al*. 2014).

Nowadays, zerovalent iron (nZVI) and magnetite nanoparticles (nMag) have been studied and used intensely because of increasing importance of magnetic nanoparticles. Various methods can be used for the production of these nanoparticles, which includes two main methods. First method is called top-down method such as vacuum sputtering (Li, Elliott *et al*. 2006) or the decomposition of iron pentacarbonyl ($Fe(CO)_5$) in organic solvents (Karlsson, Deppert *et al*. 2005); and the second method is called bottom-up method such as chemical synthesis, for example through the reaction of iron(II) or iron(III) salts with sodium borohydride (Wang and Zhang 1997, Shi, Yi *et al*. 2015). In the last few years, green chemistry synthesis for the production of nZVI has been used and green tea leaves can be given as an example due to its high antioxidant capacities (Chrysochoou, Johnston *et al*. 2012). (Machado, Pinto *et al*. 2013) compared the dried and non-dried leaves for antioxidant capacities and they found that dried leaves produced extracts with higher antioxidant capacities than non-dried leaves. The extracted compounds react with iron(III) in solution to form the nZVI. The extraction conditions were optimized by trying various parameters such as temperature, contact time, and volume: mass ratio (Machado, Pinto *et al*. 2013). Zerovalent iron nanoparticles (nZVI) have been shown in the last couple of years to be effective for environmental remediation of a large diversity of organic and inorganic contaminants available in groundwater, wastewater and drinking water. Some examples contain nitrate (Cho, Song *et al*. 2015), heavy metals (Zn, Cd, Ni, Cu and Cr) (Calderon and Fullana 2015), chlorinated organic solvents (Yan, Lien *et al*. 2013) azo-dyes (Fan, Guo *et al*. 2009, Yu, Chen *et al*. 2014) and waterborne estrogens (Jarošová, Filip *et al*. 2015).

One of the other important magnetic nanoparticle is magnetite (Fe_3O_4). Magnetite is accessible as ferrimagnetic and super paramagnetic at room temperature. Super paramagnetic behavior of iron oxide nanoparticles can be assignable to their size. When the size gets smaller than 20 nm, thermal fluctuations can change the direction of magnetization of the entire crystal (Teja and Koh 2009). Several methods have been developed up to now for synthesis of magnetite nanoparticles such as sol-gel (Sciancalepore, Rosa *et al*. 2014), thermal decomposition (Maity, Kale *et al*. 2009),co-precipitation (Khalil 2015)and hydrothermal synthesis (Ahmadi, Masoudi *et al*. 2013).Magnetite nanoparticles have several applications in the field of adsorption (Yao, Miao *et al*. 2012), medicine (Adams, Rai *et al*. 2015), heavy metal cations removal (Iwahori, Watanabe *et al*. 2014), oil removal (Liang, Du *et al*. 2015)and bacteria removal from water (Kumar, Sakthivel *et al*. 2015).

Membranes have been widely used in different industries such as medical, pharmaceutical,

chemical, food and textile. In these days, membrane processes are also used intensively for obtaining high-quality water for domestic and industrial demands, treatment and reuse of wastewater and removal of toxic components as well as recovery of valuable components from various industrial effluents (Suwal, Roblet *et al*. 2014, Bani-Melhem, Al-Qodah *et al*. 2015, Yurtsever, Sahinkaya *et al*. 2015).

Nano sized metal particles are an important class of materials due to the unique physical and chemical properties other than those from the bulk size metals. Different functional groups bring dissimilar potential applications for membrane implementation **(**Jian 2007). Recently, many studies have been focused on modification of membrane pores or surface with functional groups with nanoparticles such as Ag, TiO_2, Se, Cu, ZnO nanoparticles, and nanoscale zerovalent iron (Lee, Kim *et al*. 2008, Akar, Asar *et al*. 2013, Ma, Yu *et al*. 2015, Al-Hobaib, El Ghoul *et al*. 2015, Rehan, Gzara *et al*. 2016). At the present time, metal nanoparticles blended in polymer films or membranes have been shown great interest due to the many advantages (Ikeda, Akamatsu *et al*. 2004, Pivin, Sendova-Vassileva *et al*. 2006, Weiming, Jun *et al*. 2015, Rajabi, Ghaem *et al*. 2015).

Polyethersulphone (PES) is widely used because of its inherently hydrophilic nature that provides wetting properties of the membrane and completely resulting in fast filtration. It is the most common ones used in microfiltration/ultrafiltration of wastewater and provides removal of tiny particles, bacteria, viruses, and fungi making it a well-rounded membrane for applications such as sample preparation and sterile filtration for aqueous solutions (Karode, Gupta *et al*. 2000, Mocé-Llivina, Jofre *et al*. 2003, Basri, Ismail *et al*. 2011, Zodrow, Brunet *et al*. 2009, Rosas, Collado *et al*. 2014).

In the current work, zerovalent iron (nZVI, Fe^0) or magnetite (nMag, Fe_3O_4) nanoparticles were synthesized and used to prepare membranes with antibacterial performance for testing in the domestic wastewater treatment. So far, several studies have been performed to prepare composite membrane using different types of nanoparticles. Moreover, many researches presented in literature highlighted toxicity studies of nZVI (Lefevre, Bossa *et al*. 2016). However, to the best of our knowledge, a limited number of satisfactorily studies are available on the comparison of antibacterial activity of polyethersulfone composite membrane containing zerovalent iron or magnetite nanoparticles in the literature. Thus, the zerovalent iron and magnetite nanoparticles were synthesized and characterized by scanning electron microscopy (SEM), X-ray powder diffraction (XRD), and particle size distribution (PSD) analysis. Also, the fabricated iron nanocomposite membranes synthesized by a solution blending technique were characterized by scanning electron microscopy energy-dispersive X-ray spectroscopy (SEM-EDX), atomic-force microscopy (AFM), and pure water permeability analysis. The quantity of released iron ion to permeate streams during filtration was also analyzed. Moreover, the antibacterial activities of the nanocomposite membranes against *Escherichia coli* (*E. coli*) as the model gram-negative bacteria were tested.

2. Experimental section

2.1 Reagents

Iron(III) chloride hexahydrate ($FeCl_3.6H_2O$, Merck), iron(II) sulfate heptahydrate ($FeSO_4.7H_2O$, Merck), sodium borohydride ($NaBH_4$, Merck), hexadecyltrimethylammonium bromide ($C_{19}H_{42}BrN$, HTAB, Sigma), ethyl alcohol (C_2H_5OH, Merck) and sodium hydroxide

(NaOH, Merck) were obtained in high purity and were used as received. Polyethersulfone(PES) with a molecular weight of 58,000 g/mol (E 6020 P) was gently provided by BASF Company from Turkey. N-methyl-2-pyrrolidione (NMP) was purchased from Sigma-Aldrich. Endo-agar used in preparing plates for antimicrobial membrane filtration test was purchased from Merck. Endo agar and nutrient agar plates were prepared according to Merck Microbiology Manual 12th Ed. *E. coli* (ATCC25922) bacteria were obtained from our Biotechnology Research Laboratory for Science and Technology (Mersin, Turkey). Distilled water used in all experiments was obtained with the two-stage Millipore Direct-Q3UV purification system.

2.2 Synthesis of zerovalent iron nanoparticles

The synthesis of nZVI particles were carried out in a batch reactor by the reduction of iron ions with borohydride method with applying an inert atmosphere by using N_2 gas (Sun, Li *et al*. 2006). The stock solution of $FeCl_3 \cdot 6H_2O$ was prepared freshly with dissolved absolute ethanol to prevent the oxidation of nZVI. The solutions of $NaBH_4$ and HTAB were prepared with ultra-pure water.

Theoretically, nZVI particles form by mixing equal volumes of 0,05 M $FeCl_3.6H_2O$ and 0,2 M $NaBH_4$ according to following the reaction:

$$4Fe^{3+}_{(aq)} + 3BH_4^-{}_{(aq)} + 9H_2O_{(l)} \rightarrow 4Fe^0_{(s)} + 3H_2BO_3^-{}_{(aq)} + 12H^+_{(aq)} + 6H_{2\,(g)}$$

The borohydride solution was slowly added at 1.0 rpm addition rate into the iron chloride with a peristaltic pump (Longman BT-2j) at a vigorous stirring (~400 rpm). The iron nanoparticles were harvested using a centrifuge (Sigma 3-30 K Cooler) at 13500 rpm. The synthesized iron particles were then washed three times with absolute ethanol to prevent oxidation and dried at 70 °C for 4 hours in a vacuum oven. The samples were stored in a vacuum medium.

2.3 Synthesis of magnetite nanoparticles

The magnetite nanoparticles were synthesized through the co-precipitation method by adding a base to an aqueous mixture of Fe^{3+} and Fe^{2+} salts (Tina, Pouliot *et al*. 2013).

$$Fe^{2+} + 2Fe^{3+} + 8OH^- \rightarrow Fe_3O_4 + 4H_2O$$

At the production step 1.62 g of $FeCl_3.6H_2O$ and 1.39 g of $FeSO_4.7H_2O$ dissolved in 40 mL of water. The 5 mL of NaOH (3 N) solution slowly added ferrous solution at 70℃ during 30 min time range. The black color magnetite was produced and precipitated in reaction medium. After that 5 mL of NaOH (3 N) added in reaction medium. The magnetite nanoparticles were removed in the supernatant after centrifuge process. In the next step, nanoparticles were washed five times with ultra-pure water, centrifuged and nanoparticles were removed. The obtained magnetite nanoparticles were dried at 65℃ for 4 hours in a vacuum medium.

2.4 Characterization of zerovalent iron and magnetite nanoparticles

XRD analysis was undertaken using a Rigaku Smartlab model XRD at Cu-Kα radiation (λ=1.54 Å). The XRD analysis of dried nZVI and magnetite samples were carried out continuous scans from 10 to 100θ at 2θ scan rate at 2θ min^{-1} in ambient air. The mean hydrodynamic diameters of the iron nanoparticles were determined using DLS. Obtained fresh nZVI and magnetite particles were dispersed in water with Sigma 3-30 K Cooling Centrifuged ultrasound

Table 1 The casting solution composition of the synthesized membranes (composition in wt%.)

Membrane sample	PES	NMP	Nano-iron
Pristine PES	14	86.00	0.00
PES/nZVI-0.25	14	85.75	0.25
PES/nZVI-0.50	14	85.50	0.50
PES/nZVI-1.00	14	85.00	1.00
PES/nMag-0.25	14	85.75	0.25
PES/nMag-0.50	14	85.50	0.50
PES/nMag-1.00	14	85.00	1.00

equipment then hydrodynamic diameters of nanoparticles were measured at 25℃, using a Malvern 2000 Zetasizer Nano ZS90. Images of nZVI and magnetite nanoparticles were recorded with a Zeiss Supra 55 SEM.

2.5 Synthesis of pristine PES membrane

Pristine PES membranes were synthesized by a wet phase inversion method. The PES beads was dried in an oven at 80℃ for 2 h. Casting solution was prepared by dissolving PES beads (14% w/w) in NMP solvent. The composition of casting solution employed for the fabrication of membrane is described in Table 1. The prepared solution was stirred vigorously at 60℃ for 6 h and then agitated at room temperature over night to obtain a clear homogenous solution. Afterwards, the polymer solution was ultrasonicated 20 min to remove air bubbles from the solutions. The bubble-free solution was cast onto a glass plate with a cast knife of about 200 μm gap at 100 mm/s. The casting films were kept 10 s for evaporation, and the glass plate was immediately immersed into a coagulation bath containing distilled water. After coagulation, PES membranes were separated from the glass plate and membranes were stored in distilled water for 1 day to guarantee the complete phase inversion. Thickness of the prepared membranes was measured by a digital micrometer as 160±20 μm.

2.6 Synthesis of nanoparticles blended composite PES membrane

Zerovalent iron and magnetite nanoparticles blended membranes were synthesized according to the phase inversion method. In this method, the iron nanoparticles were added to the casting solution. Different ratios of nZVI or nMag particles were dispersed in NMP solvent using an ultrasonication bath for 30 min and PES beads were then added to this solution. Then, the casting solutions of PES/nZVI or PES/nMag membranes were obtained in Section 2.5.

2.7 Characterization of composite membranes

The surface and cross-section morphology of the synthesized membranes were investigated by SEM-EDX using a Zeiss/Supra 55 FE-SEM model operating at 10 kV. For the cross-section image, the PES membranes were fractured after immersion in liquid nitrogen. All samples were dried and coated under vacuum with a thin layer of platinum-palladium by a sputtering system.

The AFM analyses were performed on an AFM microscope (Park System XE-100 SPM). Small

squares (0.5×0.5 mm) of dried samples were cut and fixed on a glass plate and 5 μm×5 μm areas were scanned. At least three different locations were measured, and the average values of the surface roughness (R_a) were presented.

The filtration performance of the prepared membranes was measured by a dead-end membrane module (Sterlitech HP4750 stirred cell) with a filtration area of 14.6 cm^2 at a temperature of 25℃ and an operating pressure of 1.5 bar.

The permeation flux (J) was measured by collecting the filtered water in the determined intervals and calculated using the following Eq. (1)

$$J = \frac{V}{A \times \Delta t} \tag{1}$$

where, J is permeate flux (L/m^2h); V the volume of permeate pure water (L), A the effective area of the membrane (m^2), and Δt the permeation time (h).

The membrane porosity (ε) was determined by gravimetric method, as defined in the following Eq. (2) (Li, Xu *et al*. 2009, Vatanpour, Madaeni *et al*. 2012)

$$\varepsilon = \frac{W_w - W_d}{\rho_w \times A \times \ell} \times 100 \tag{2}$$

where, W_w is the weight of the wet membrane (g); W_d the weight of the dry membrane (g); ρ_w the density of pure water at room temperature (0.998 g/cm^3); A the effective area of the membrane (cm^2), and l the membrane thickness (cm).

Furthermore, the mean pore radius (r_p) on the basis of the pure water flux and porosity data was determined using the filtration velocity method. According to the Guerout-Elford-Ferry equation, r_p could be determined by the following Eq. (3) (Li, Xu *et al*. 2009, Vatanpour, Madaeni *et al*. 2012)

$$r_p = \sqrt{\frac{(2.9 - 1.75\varepsilon) 8\eta \ell Q}{\varepsilon \times A \times \Delta P}} \tag{3}$$

Where r_p is mean pore radius (nm); η water viscosity (8.9×10^{-4} Pa s); l the membrane thickness (m); Q the volume of the permeate water per unit time (m^3/s); ΔP the operating pressure (0.15 MPa).

The amount of iron released from the membranes during the filtration test in the permeate stream was also measured by an atomic absorption spectroscopy (AAS) (Agilent 7500CE, Japan).

2.8 Microbial experimentation and antibacterial activity of membranes

The antibacterial activity of the composite membranes containing nZVI or nMag particles against *E. coli* bacteria was carried out by agar diffusion method. Bacteria were grown aerobically on agar plates at 37℃ overnight. Nutrient and Endo agar cup plate methods were conducted to determine antibacterial activity of the nZVI or nMag particles against the test pathogen *E. coli*. To determine the inhibition effect of iron nanoparticles on *E. coli* growth, 10 mm diameters of iron pellets were placed on the plates and were incubated at 37℃ for 24 h. The zone of growth inhibition around each pellet after the incubation period, confirms the antimicrobial activity of the nZVI and nMag particle pellets (each pellets were 250 mg weight). However, 100 mL of *E. coli* solution was filtered using dead-end filtration system and at the end of filtration, membrane was

put on the agar in order to test antibacterial activity of composite membranes. The pristine PES membrane was considered as the control sample.

3. Results and discussion

3.1 Characterization of zerovalent iron and magnetite nanoparticles

3.1.1 X-Ray diffraction (XRD)

The XRD pattern of nZVI and nMag samples is given in Figs. 1(a)-(b), respectively. Fig. 1(a) indicates that the characteristic basic reflection of Fe^0 state at 45.23° and no signals for iron oxides at about 2 theta of 36°. This result showed that iron present in the sample was mainly in its zerovalent state. As can be seen at Fig. 1(b), the basic reflection of Fe_3O_4 appearing at 2 theta of 35.62°.

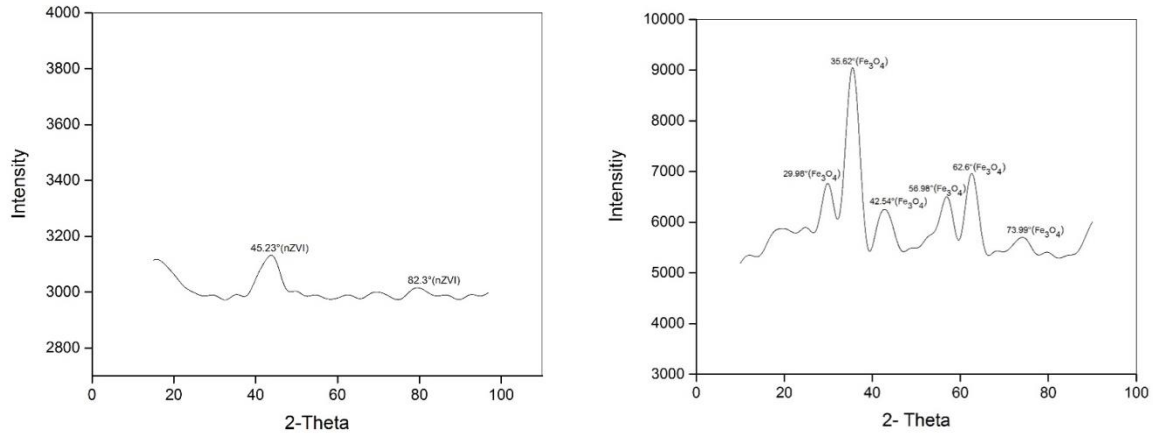

(a) (b)

Fig. 1 XRD pattern of (a) nZVI and (b) nMag particles

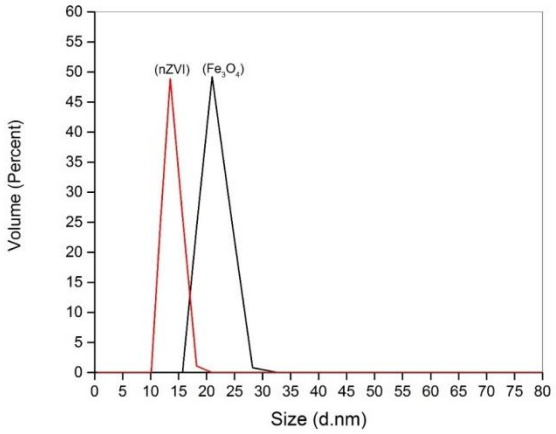

Fig. 2 PSD of nZVI and nMag particles

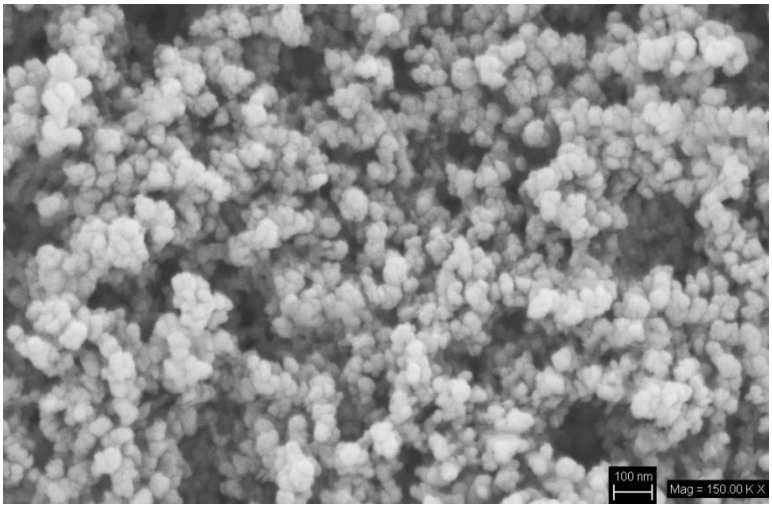

(a)

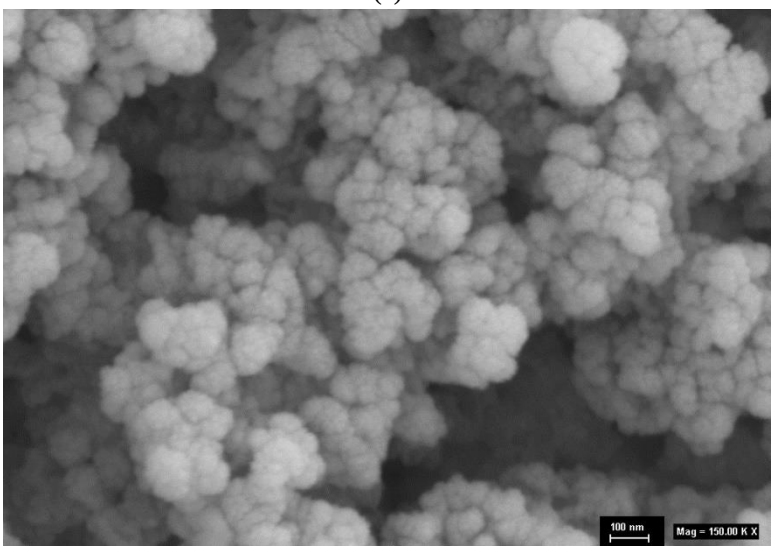

(b)

Fig. 3 SEM images of (a) nZVI and (b) nMag particles

3.1.2 Particle size distribution (PSD)

Fig. 2 shows the PSD of the synthesized nZVI and nMag particles. The mean diameter of nZVI was 13.71 nm (100%volume, standard deviation 1.49 nm), and also the mean diameter of nMag was 21.26 nm (100%volume, standard deviation 2.29 nm). Thereby, the PSD results showed that synthesized iron particles were of nanoscale diameter.

3.1.3 Scanning electron microscopy (SEM)

Typical SEM images of nZVI and nMag particles are shown in Figs. 3(a)-(b), respectively. Fig. 3(a) indicates the nZVI, which formed chain-like structure. Also the Fig. 3(b) shows the image of nMag, which formed bunch of grape-like structures.

Table 2 Effect of nano-iron amount on the water flux, pore size, and porosity properties

Membrane sample	Pure water flux (L/m^2h)	Mean pore radius (nm)	Porosity (%)	Released iron in permeate (µg/L)
Pristine PES	58±2.7	20.2±0.2	56.83±3.15	-
PES/nZVI-0.25	110±3.2	27.5±0.1	60.99±4.32	90
PES/nZVI-0.50	160±5.4	33.3±0.2	64.20±3.78	102
PES/nZVI-1.00	189±6.2	34.6±0.1	68.94±2.86	122
PES/nMag-0.25	207±4.4	34.4±0.2	60.05±3.95	108
PES/nMag-0.50	246±5.9	38.6±0.1	61.04±4.14	231
PES/nMag-1.00	305±6.7	40.9±0.2	63.32±5.32	396

3.2 Characterization of pristine PES and PES/nZVI or PES/nMag composite membranes

The pure water flux, mean pore radius and porosity of the pristine and composite membranes are presented in Table 2. The results indicated that pore size of the pristine PES membrane was approximately in the range of ultrafiltration membranes (20.2±0.2 nm). It can be clearly seen that the water flux, pore radius, and porosity of the composite membranes were higher than the pristine membrane. So, it can be deduced that the blending of iron into the membranes had significant effect on the membrane morphology. The porosity of nZVI membranes close to the porosity of nMag membranes despite radius mean pore values of nZVI membranes were higher. Also, it can be concluded that the composite membranes had higher flux and bigger pore size when compared with the pristine PES membrane. As shown in Table 2, the composite membrane prepared with 0.25%wt. nZVI had the lowest water flux whereas 1.0%wt. nMag had the highest flux. It can be explained as the pore size of nMag membranes had greater than the pore size of nZVI membranes. Furthermore, the amount of iron released during the filtration process was determined by the AAS analysis (Table 2). nMag membranes released higher iron ion when compared with nZVI membranes.

Fig. 4 shows the morphologies of top-layer and cross-section of the membranes. Pristine membrane had a dense skin layer (Figs. 4(a)-(h)). It can be clearly observed from the SEM images that the iron nanoparticles are blended homogeneously in the polymer matrix. The nanoparticles on the membrane surface increased with the increase of iron-nanoparticles amount (Figs. 4(b) to (g)). The addition of nanoparticles also affected the structures of the cross-section (Figs. 4i to 4n). However, nanocomposite membrane which has the finger-like structure demonstrated wider pore size, which would enhance the extra permeation flux of the membrane when compared with pristine PES membrane. Additionally, most of the nano-iron particles settled on the surface PES membrane were as round shaped. But, the shape of the magnetite nanoparticles (Figs. 4e to 4g) was homogeneous than the iron nanoparticles (Figs. 4(b) to (d)). As shown in Fig. 4(a), no nanoparticles were observed on the pristine membrane and some nanoparticles were detected on the surface of composite membranes (Figs. 4(b) to (g)). These observations were also supported with the EDX analysis as shown in Fig. 5. These images proved that iron nanoparticles were successfully penetrated in the polymer matrix (Figs. 5(a) to (e)). The iron peak was observed all of the composite membranes.

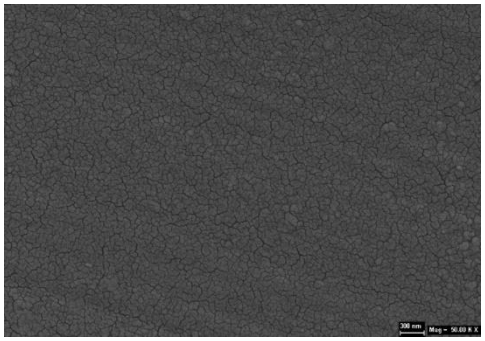

(a) Pristine PES

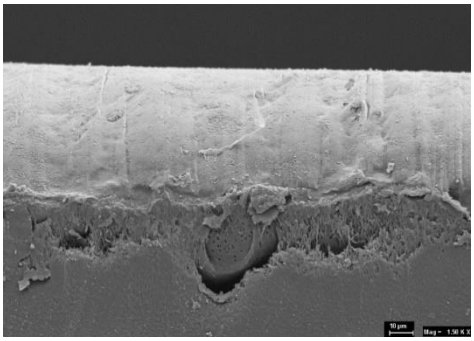

(h) Pristine PES

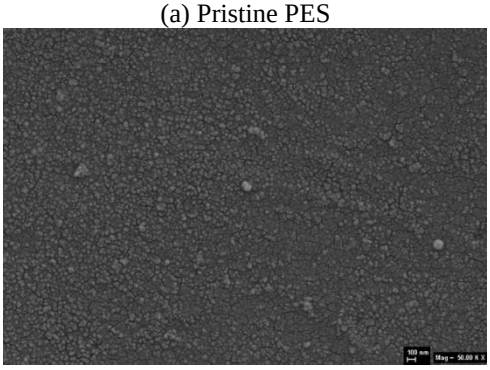

(b) PES/nZVI-0.25

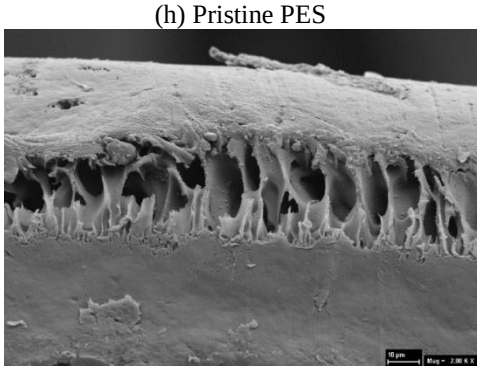

(i) PES/nZVI-0.25

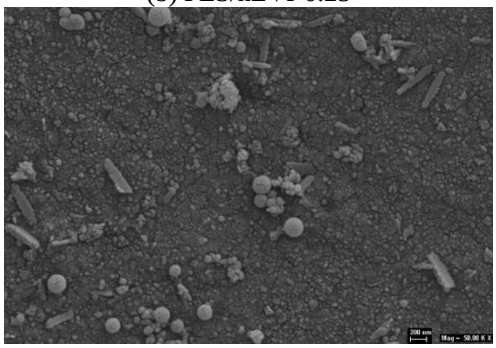

(c) PES/nZVI-0.50

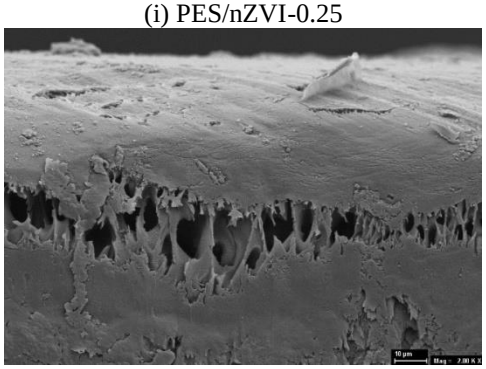

(j) PES/nZVI-0.50

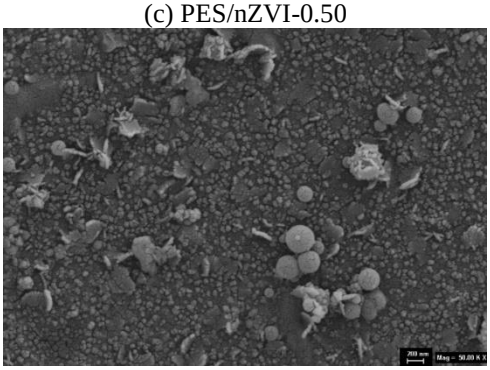

(d) PES/nZVI-1.00

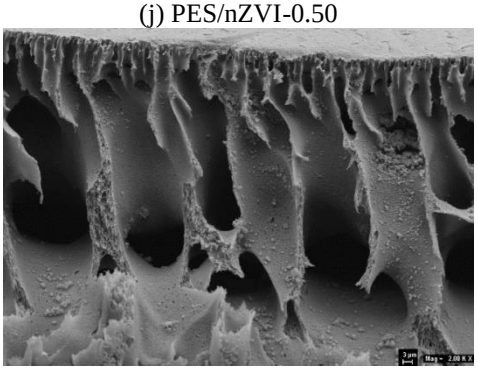

(k) PES/nZVI-1.00

Fig. 4 SEM images from the surface and cross-section of the (a,h) pristine PES membrane, (b,i) PES/nZVI-0.25, (c,j) PES/nZVI-0.50, (d,k) PES/nZVI-1.0, (e,l) PES/nMag-0.25, (f,m) PES/nMag-0.50, (g,n) PES/nMag-1.00

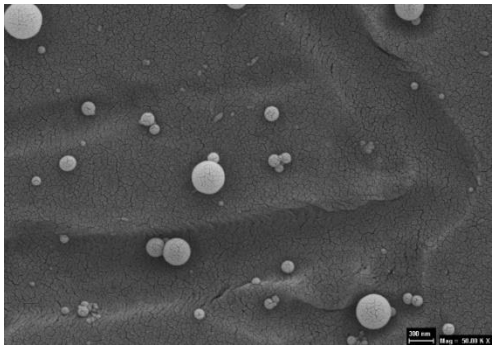

(e) PES/nMag-0.25

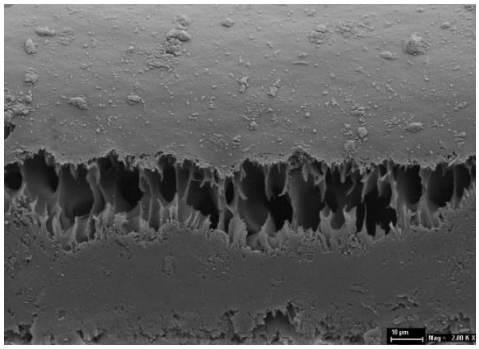

(l) PES/nMag-0.25

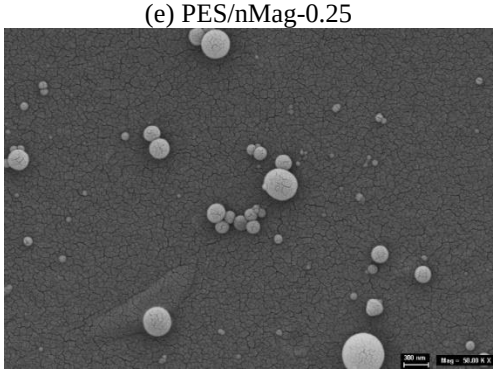

(f) PES/nMag-0.50

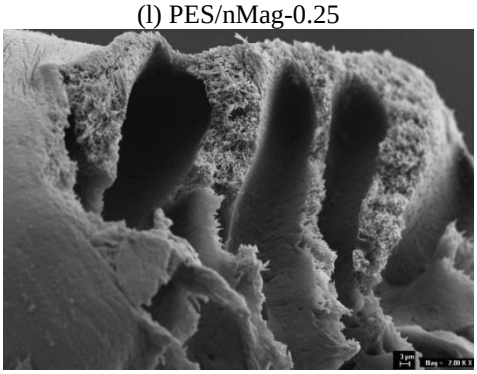

(m) PES/nMag-0.50

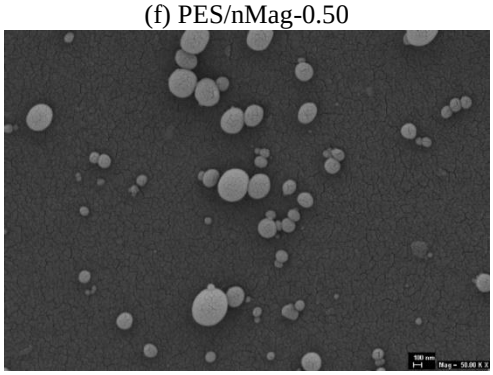

(g) PES/nMag-1.00

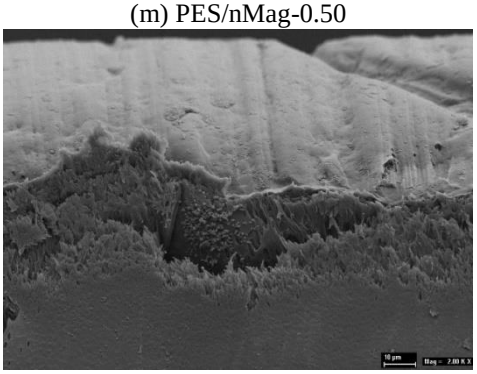

(n) PES/nMag-1.00

Fig. 4 Continued

The AFM analysis was used to investigate the changes on surface morphology and roughness of the composite membranes. The three-dimensional AFM topography images of the pristine, PES/nZVI, and PES/nMag membranes are shown in Fig. 6. The roughness (R_a) values of different membranes are presented in Table 3. Nano-iron aggregates on the membrane surface cause an increase in roughness which is beneficial for anti-biofouling performance (Rehan, Gzara *et al*. 2016). The AFM images of the composite membranes (Figs. 6(b) to (g)) indicate that the surface roughness of these membranes was higher than the pristine PES membrane (Fig. 6(a)). It can be seen that the iron concentration affected the surface roughness of the composite membrane. The nZVI and nMag concentration increased from 0.25 to 1.0%wt., the R_a value increased from 9.83±0.25 to 13.24±0.52nm and from 9.76±0.36 to 11.36±0.48 nm, respectively. The roughness

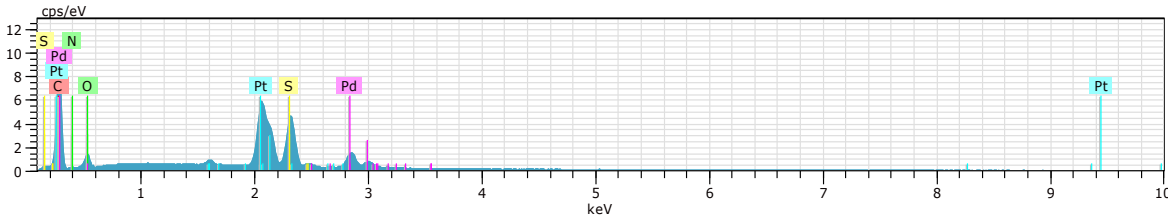

(a) Pristine PES

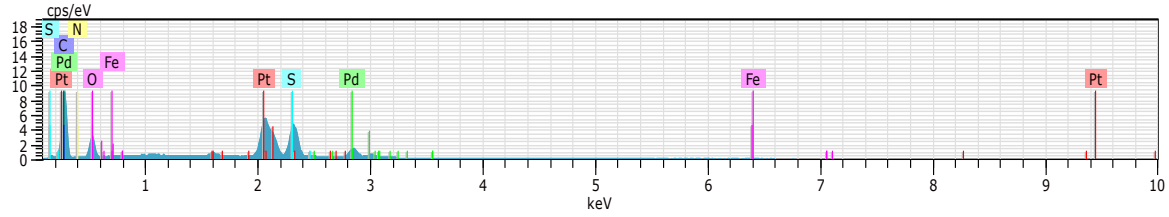

(b) PES/nZVI-0.25

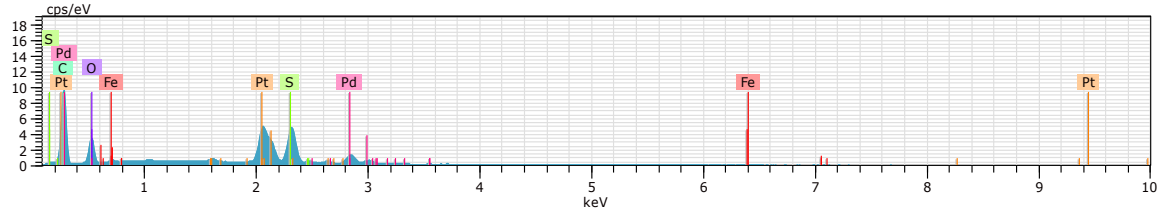

(c) PES/nZVI-0.50

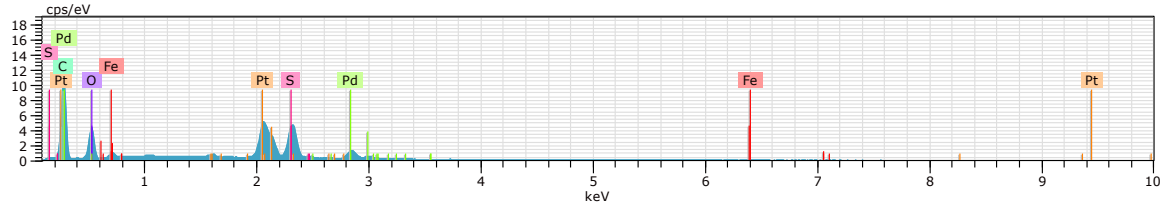

(d) PES/nZVI-1.00

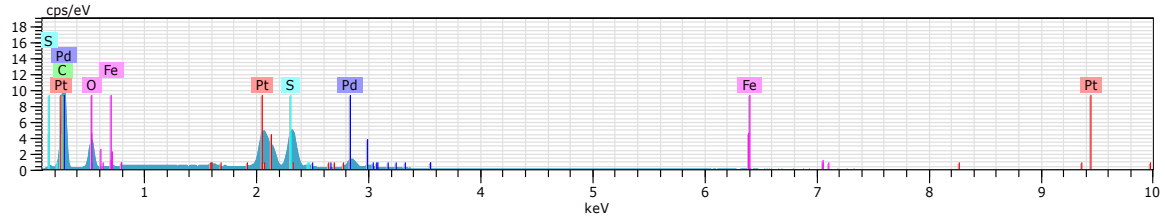

(e) PES/nMag-0.25

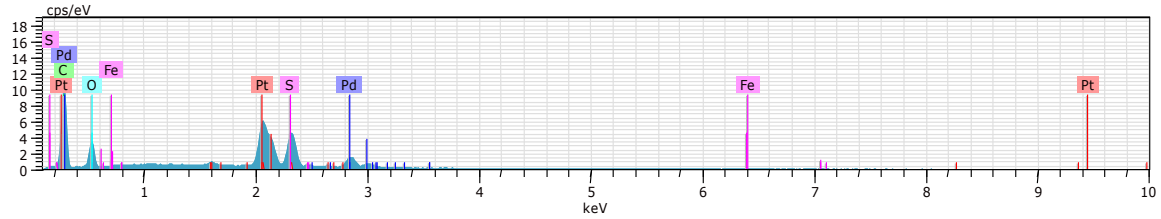

(f) PES/nMag-0.50

Fig. 5 EDX images from the surface of the (a) pristine PES membrane, (b) PES/nZVI-0.25, (c) PES/nZVI-0.50, (d) PES/nZVI-1.0, (e) PES/nMag-0.25, (f) PES/nMag-0.50, (g) PES/nMag-1.00

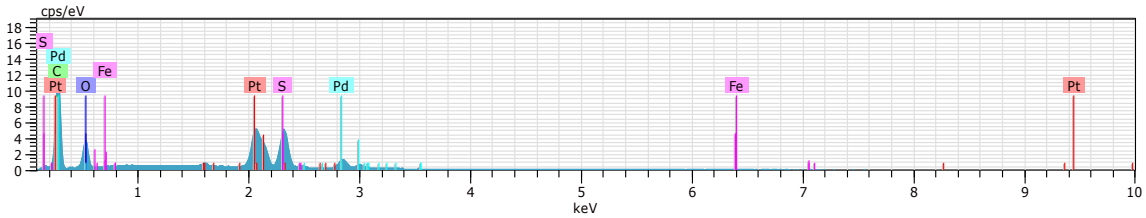

(g) PES/nMag-1.00

Fig. 5 Continued

values of the membranes containing nZVI were higher than nMag blended membranes because of the more heterogeneous surface than nMag nanocomposite membranes. Similar results were observed by (Toroghi, Raisi *et al*. 2014).

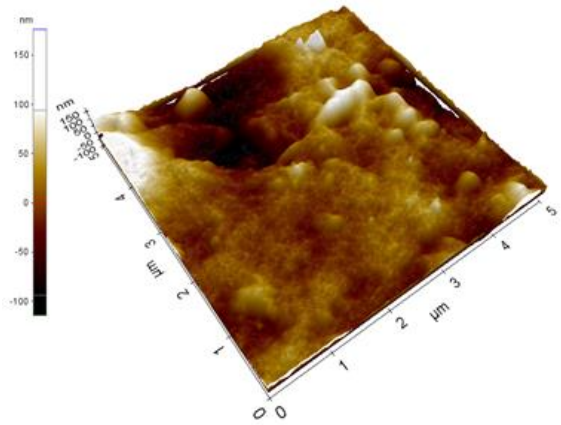

(a) Pristine PES

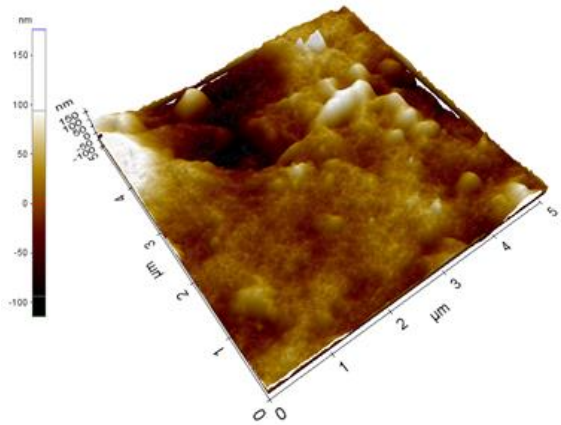

(a) Pristine PES

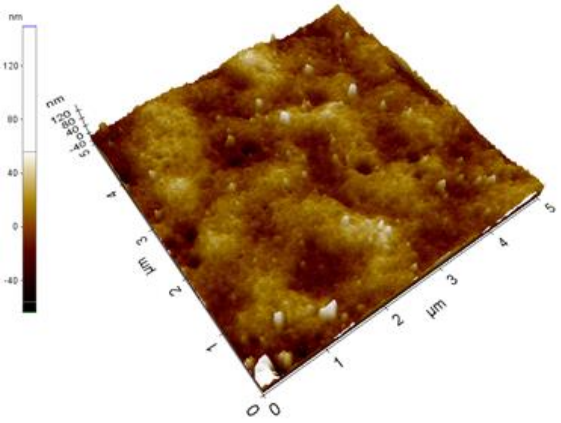

(b) PES/nZVI-0.25

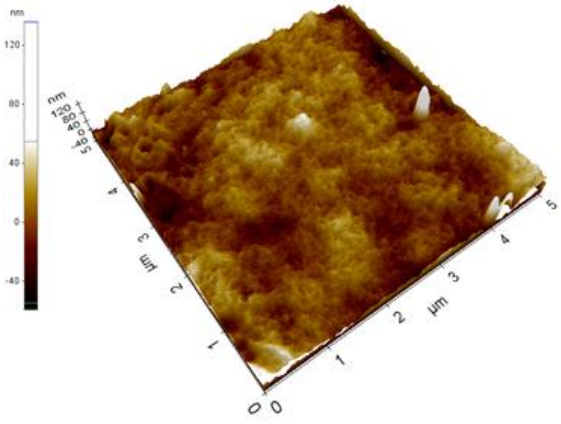

(e) PES/nMag-0.25

Fig. 6 AFM images from the surface of the (a) pristine PES membrane, (b) PES/nZVI-0.25, (c) PES/nZVI-0.50, (d) PES/nZVI-1.00, (e) PES/nMag-0.25, (f) PES/nMag-0.50, (g) PES/nMag-1.00

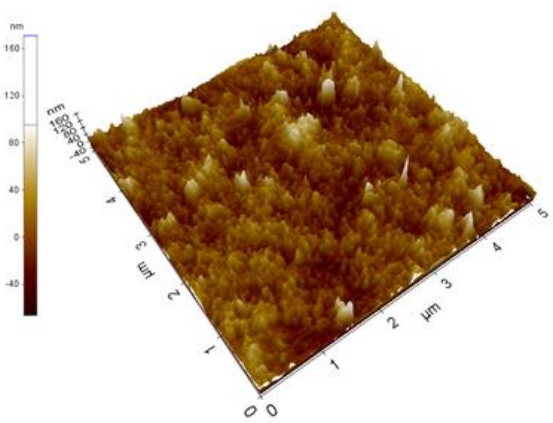

(c) PES/nZVI-0.50

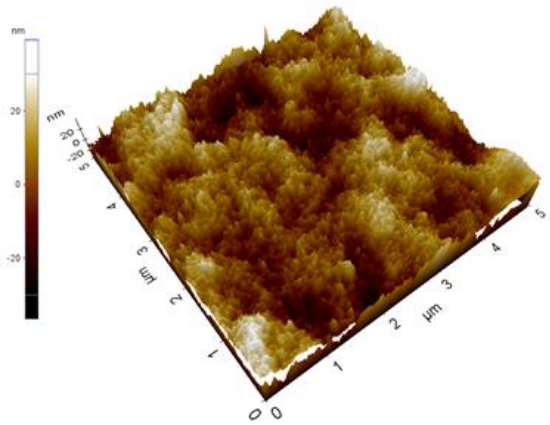

(f) PES/nMag-0.50

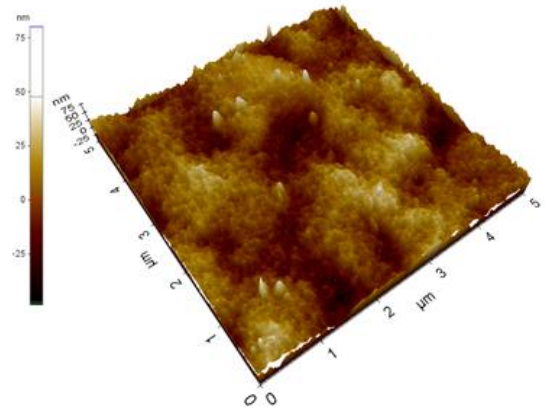

(d) PES/nZVI-1.00

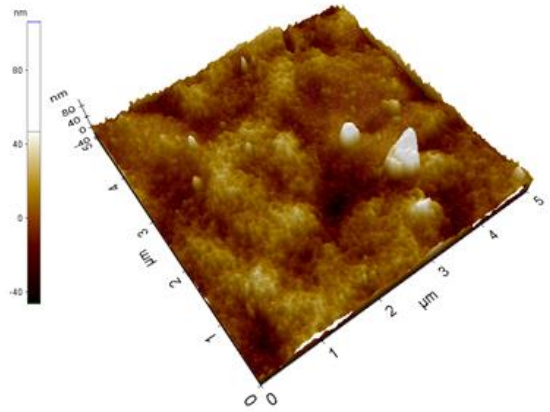

(g) PES/nMag-1.00

Fig. 6 Continued

Table 3 $R_a$values of different membranes

Membrane sample	R_a (nm)
Pristine PES	7.64±0.29
PES/nZVI-0.25	9.83±0.25
PES/nZVI-0.50	12.78±0.31
PES/nZVI-1.00	13.24±0.52
PES/nMag-0.25	9.76±0.36
PES/nMag-0.50	10.52±0.53
PES/nMag-1.00	11.36±0.48

3.3 Antibacterial activity of pristine, nZVI and nMag composite PES membranes

Fig. 7 shows the agar disc diffusion test against *E. coli*. The nZVI pellets supplied satisfactory antibacterial activity with inhibition zone of 24 mm; however, nMag particle pellets did not show

Fig. 7 (a) Control sample, (b) inhibitory zones of the nZVI pellets, (c) inhibitory zones of the nMag pellets

any antimicrobial activity against *E.coli* (gram negative) (Fig. 7). nZVI nanoparticles successfully inhibit *E. coli* growth on nutrient and endo agar media. This is supported by recent studies (Li, Greden *et al*. 2010, Qiu, Fang *et al*. 2013, Jang, Lim *et al*. 2014). However, the nMag particles did not show any activity against *E.coli*. There are many factors responsible for the antibacterial activity of nZVI particles. The main mechanism might be via oxidative stress generated by reactive oxygen species (ROS) (such as superoxide radicals (O^{2-}), hydroxyl radicals (-OH), hydrogen peroxide (H_2O_2), and singlet oxygen ($^1O_2$) which can destroy the proteins and DNA in bacteria (Sies 1997, Auffan, Achouak *et al*. 2008). Metallic iron (Fe^0) created a source of ROS leading to the inhibition of *E.coli*. (Kim, Kuk *et al*. 2007) reported that H_2O_2 reacted with ferrous irons via the Fenton reaction and produced hydroxyl radicals which are known to damage biological macromolecules. Moreover, some authors have demonstrated that the small size of nanoparticles can cause bactericidal effects. For example, (Lee, Im *et al*. 2008) proved that the inhibition of *Escherichia coli* by zerovalent iron nanoparticles could be due to penetration of the small particles (10-80 nm) into *E. coli* membranes.

Antibacterial activity of the membranes was tested by the agar diffusion method using *E. coli*. In the present study, PES/iron nanocomposite membranes exhibit an interesting antibacterial performance. The colonies of *E. coli* bacteria could not be detected in the clear zone directly around the membrane samples. This clear zone indicates the antibacterial efficiency of these membranes, while there was no clear zone for the control sample. The bacterial inhibition indicated that released iron ion from the membranes diffused into the agar layer and prevented the growth of microbial colonies in the agar medium. However, PES/nZVI blended membranes showed better antibacterial activity when compared with PES/nMag composite membranes. (Behera, Patra *et al*. 2012), reported that iron oxide (Fe_3O_4) nanoparticles showed better bactericidal activity in Gram-positive bacteria as compared to Gram-negative bacteria. The antibacterial activity of iron oxide nanoparticle enhanced moderate antimicrobial activity against some pathogenic strains with zone of inhibition ranging from 9 to 22 mm (Behera, Patra *et al*. 2012).

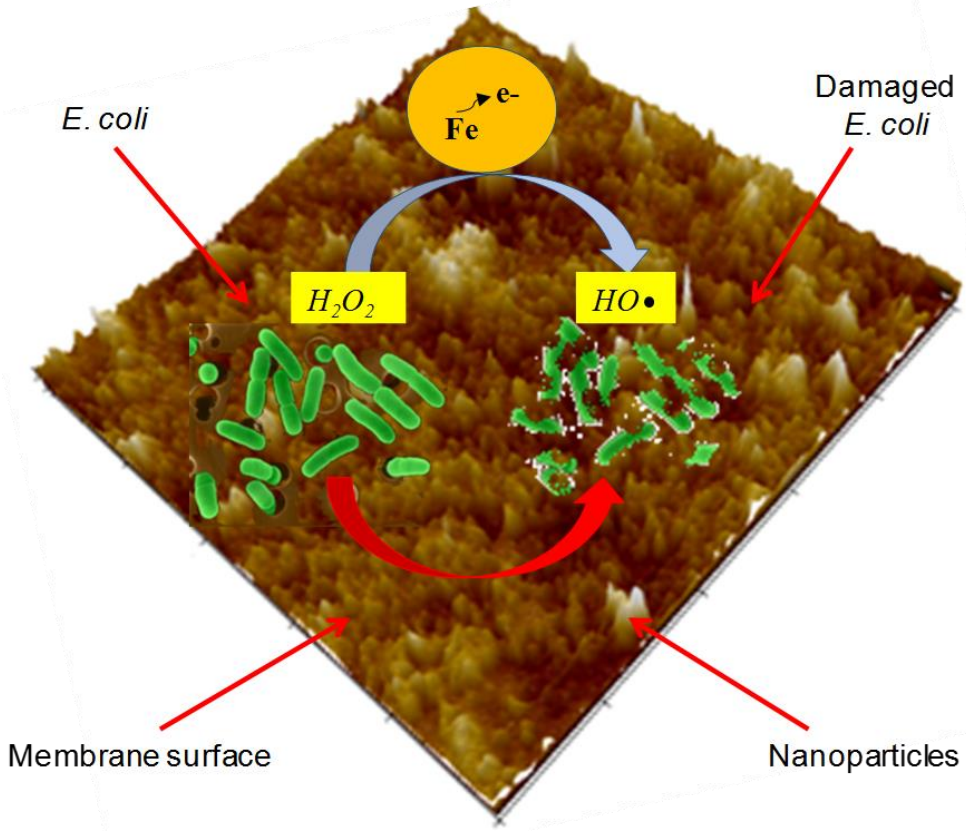

Fig. 8 Antibacterial draft map of the nanocomposite membrane

Table 4 Comparison of antibacterial activity for different membranes

Membrane	Antibacterial agent	Antibacterial efficiency	References
PES	Blending nZVI and nMag	Muchless *E. Coli* growth on the surface	This study
PES	Blending Cu^{2+}-HNTs	100% (bacteriostasis rate)	Chen, Zhang *et al.* (2012)
PVDF	Blending TiO_2 particles	Removal almost complete of *E. coli* within 1 min of UV light exposure	Damodar, You *et al.* (2009)
PVDF	Fullerene (C60) nanoparticles	Much less bacterial growth on the surface	Kim, Lee *et al.* (2015)
PS	Silver nanoparticles	Much less bacterial growth on the surface	Taurozzi, Arul *et al.* (2008)

It is observed that very few bacteria were found in the membrane permeate when used PES/nZVI composite membranes. However, some of the bacteria were alive when used PES/nMag composite membranes. As a result, nZVI blended membranes fairly showed better antibacterial activity performance than the nMag blended membranes.

The antibacterial mechanism of the PES/nZVI composite membranes, as shown in Fig. 8, could be interpreted as follows: The loaded iron ions on membrane surfaces could absorb onto the

surface of bacteria cells and further damage the cell membrane (Dan, Ni *et al*. 2005, Liu, Hsieh *et al*. 2009, Ö zdemir, Limoncu *et al*. 2010).

The comparison of antibacterial activity of the membranes with other antibacterial agents showed that PES/nZVI composite membranes also had good antibacterial property (Table 4). Thus, the synthesized nanocomposite membranes will have a potential application to treat wastewater containing *E.coli* for reducing biofouling

4. Conclusions

The nZVI and nMag particles were synthesized and blended with different concentration into PES membranes via phase inversion method. XRD analysis of nZVI and nMag showed that the basic reflection of Fe^0 and Fe_3O_4 were observed. Moreover, PSD analysis demonstrated that the size of nZVI and nMag particles were 13.71 and 21.26 nm, respectively. SEM images showed that chain-like structure and grape-like structures were obtained for nZVI and nMag particles, respectively. The effects of nZVI and nMag particles amount when blended with PES membranes were investigated by pure water flux, mean pore radius, porosity, and antibacterial activity. The results showed that the water flux, pore radius, and porosity of the composite membranes were higher than the pristine membrane. SEM images of membranes showed typical asymmetric structure. AFM results demonstrated that the surface roughness (R_a) increased with the increase in nano-iron amount. All the PES/nZVI membranes showed better antibacterial activity than PES/nMag composite membranes. The antibacterial test indicated that nZVI in the PES membranes could be an effective way to control membrane bio-fouling. They would have a potential application to reduce bacterial fouling at membrane treatment of wastewater.

The durability of the antibacterial activity of the nanoparticles and the prepared membranes are important subject in order to control membrane fouling. Further investigation of the long-term durability should be carried out to consider sustainability of this product and its economic feasibility. Efforts should continue on the development of membranes which have long-term antibacterial effects.

References

Abhilash, M. (2010), "Potential applications of nanoparticles", *Int. J. Pharma Bio Sci.*, **1**(1), 1-12.

Adams, C.F., Rai, A., Sneddon, G., Yiu, H.H., Polyak, B. and Chari, D.M. (2015), "Increasing magnetite contents of polymeric magnetic particles dramatically improves labeling of neural stem cell transplant populations", *Nanomed. Nanotech. Biology Med.*, **11**(1), 19-29.

Ahmadi, R., Masoudi, A., Hosseini, H.R.M. and Gu, N. (2013), "Kinetics of magnetite nanoparticles formation in a one-step low temperature hydrothermal process", *Ceram. Int.*, **39**(5), 4999-5005.

Akar, N., Asar, B., Dizge, N. and Koyuncu, I. (2013), "Investigation of characterization and biofouling properties of PES membrane containing selenium and copper nanoparticles", *J. Membrane Sci.*, **437**, 216-226.

Al-Hobaib, A.S., El Ghoul, J. and El Mir, L. (2015), "Synthesis and characterization of polyamide thin-film nanocomposite membrane containing ZnO nanoparticles", *Membrane Water Treat.*, **6**(4), 309-321.

Auffan, M., Achouak, W., Rose, J., Roncato, M., Chanéac, C., Waite, D.T., Masion, A., Woicik, J.C., Wiesner, M.R. and Bottero, J. (2008), "Relation between the redox state of iron-based nanoparticles and their cytotoxicity toward Escherichia coli", *Environ. Sci. Technol.*, **42**, 6730- 6735.

Ayyappan, S., Philip, J. and Raj, B. (2009), "Solvent polarity effect on physical properties of CoFe2O3 nanoparticles", *J. Phys. Chem. C*, **113**, 590-596.
Bani-Melhem, K., Al-Qodah, Z., Al-Shannag, M., Qasaimeh, A., Qtaishat, M.R. and Alkasrawi, M. (2015), "On the performance of real grey water treatment using a submerged membrane bioreactor system", *J. Membrane Sci.*, **476**, 40-49.
Basri, H., Ismail, A.F. and Aziz, M. (2011), "Polyethersulfone (PES) ultrafiltration (UF) membranes loaded with silver nitrate for bacteria removal", *Membrane Water Treat.*, **2**(1), 25-37.
Behera, S.S., Patra, J.K., Pramanik, K., Panda, N. and Thatoi, H. (2012), "Characterization and evaluation of antibacterial activities of chemically synthesized iron oxide nanoparticles", *World J. Nano Sci. Eng.*, **2**, 196-200.
Calderon, B. and Fullana, A. (2015), "Heavy metal release due to aging effect during zero valent iron nanoparticles remediation", *Water Res.*, **83**, 1-9.
Chen, L., Kong, W., Yao, J., Zhang, H., Gao, B., Li, Y., Bu, H., Chang, A. and Jiang, C. (2015), "Synthesis and characterization of Mn-Co-Ni-O ceramic nanoparticles by reverse micro emulsion method", *Ceram. Int.*, **41**(2), 2847-2851.
Chen, Y., Zhang, Y., Liu, J., Zhang, H. and Wang, K. (2012), "Preparation and antibacterial property of polyethersulfone ultrafiltration hybrid membrane containing halloysite nanotubes loaded with copper ions", *Chem. Eng. J.*, **210**, 298-308.
Cheng, P., Huang, Z.G., Zhuang, Y., Fang, L.C., Huang, H., Deng, J., Jiang, L.L., Yu, K.K., Li, Y. and Zheng, J.S. (2014), "A novel regeneration-free E. coli O157:H7 amperometric immunosens or based on functionalised four-layer magnetic nanoparticles", *Sens. Actuat. B: Chem.*, **204**, 561-567.
Cho, D.W., Song, H., Schwartz, F.W., Kim, B. and Jeon, B.H. (2015), "The role of magnetite nanoparticles in the reduction of nitrate in ground water by zero-valent iron", *Chemosp.*, **125**, 41-49.
Chrysochoou, M., Johnston, C.P. and Dahal, G.A. (2012), "Comparative evaluation of hexavalent chromium treatment in contaminated soil by calcium polysulfide and green-tea nanoscale zero-valentiron", *J. Hazard Mater*., **201**, 33-42.
Colombo, M., Carregal-Romero, S., Casula, M.F., Gutiérrez, L., Morales, M.P., Böhm, I.B. and Parak, W.J. (2012), "Biological applications of magnetic nanoparticles", *Chem. Soc. Rev.*, **41**(11), 4306-4334.
Damodar, R.A., You, S.J. and Chou, H.H. (2009), "Study the self-cleaning, antibacterial and photocatalytic properties of TiO2 entrapped PVDF membranes", *J. Hazard. Mater*., **172**, 1321-1328.
Dan, Z.G., Ni, H.W., Xu, B.F., Xiong, J. and Xiong, P.Y. (2005), "Microstructure and antibacterial properties of AISI 420 stainless steel implanted by copper ions", *Thin Solid. Film.*, **492**, 93-100.
Fan, J., Guo, Y., Wang, J. and Fan, M. (2009), "Rapid decolorization of azo dye methyl orange in aqueous solution by nanoscale zero valent iron particles", *J. Hazard. Mater.*, **166**(2), 904-910.
Grass, R.N., Athanassiou, E.K. and Stark, W.J. (2007), "Covalently functionalized cobalt nanoparticles as a platform for magnetic separations in organic synthesis", *Angew. Chem. Int. Ed*., **46**(26), 4909-4912.
Hufschmid, R., Arami, H., Ferguson, R.M., Gonzales, M., Teeman, E., Brush, L.N., Browning, N.D. and Krishnan, K.M. (2015), "Synthesis of phase-pure and monodisperse iron oxide nanoparticles by thermal decomposition", *Nanoscale*, **7**(25), 11142-11154.
Ikeda, S., Akamatsu, K., Nawafune, H., Nishino, T. and Deki, S. (2004), "Formation and growth of copper nanoparticles from ion-doped precurs or polyimide layers", *J. Phys. Chem. B.*, **108**, 15599-15607.
Iniyavan, P., Balaji, G.L., Sarveswari, S. and Vijayakumar, V. (2015), "CuO nanoparticles: synthesis and application as an efficient reusable catalyst for the preparation of xanthenesubstituted 1,2,3-triazoles via click chemistry", *Tetrahedron Lett.*, **56**(35), 5002-5009.
Iwahori, K., Watanabe, J.I., Tani, Y., Seyama, H. and Miyata, N. (2014), "Removal of heavy metal cations by biogenic magnetite nanoparticles produced in Fe (III)-reducing microbial enrichment cultures", *J. Biosci. Bioeng.*, **117**(3), 333-335.
Jang, M.H., Lim, M. and Hwang, Y.S. (2014), "Potential environmental implications of nanoscale zero-valent iron particles for environmental remediation", *Environ. Hlth. Toxicol.*, **29**, 1-9.
Jarošová, B., Filip, J., Hilscherová, K., Tuček, J., Šimek, Z., Giesy, J.P. and Bláha, L. (2015), "Can zero-valent iron nanoparticles remove water bornee strogens?", *J. Environ. Manage.*, **150**, 387-392.

Jian, X. (2007), "Synthesis and reactivity of membrane-supported bimetallic nanoparticles for pcb and trichloroethylene dechlorination", University of Kentucky Doctoral Dissertations, Paper 561.
Karlsson, M.N.A., Deppert, K., Wacaser, B.A., Karlsson, L.S. and Malm, J.O. (2005), "Size-controlled nanoparticles by thermal cracking of iron pentacarbonyl", *Appl. Phys. A Mater. Sci. Proc.*, **80**, 1579-83.
Karode, S.K., Gupta, B.B. and Courtois, T. (2000), "Ultrafiltration of raw Indian sugar solution using polymeric and mineral membranes", *Sep. Sci. Technol*., **35**(15), 2473-2483.
Khalil, M.I. (2015), "Co-precipitation in aqueous solution synthesis of magnetite nanoparticles using iron (III) salts as precursors", *Arab. J. Chem.*, **8**(2), 279-284.
Kim, J.S., Kuk, E. and Yu, K.N. (2007), "Antimicrobial effects of silver nanoparticles, nanomedicine: nanotechnology", *Biol. Med.*, **3**(1), 95-101.
Kim, K.H., Lee, J.S., Hong, H.P., Han, J.Y., Park, J.W. and Min, B.R. (2015), "The effect of Fullerene (C60) nanoparticles on the surface of PVDF composite membrane", *Membrane Water Treat.*, **6**(5), 423-437.
Kumar, R., Sakthivel, R., Behura, R., Mishra, B.K. and Das, D. (2015), "Synthesis of magnetite nanoparticles from mineral waste", *J. Alloy. Compound.*, **645**, 398-404.
Lee, C., Kim, J.Y., Lee, W.I., Nelson, K.L., Yoon, J. and Sedlak, D.L. (2008), "Bactericidal effect of zero-valent iron nanoparticles on Escherichia coli", *Environ. Sci. Tech.*, **42**(13), 4927-4933.
Lee, H.S., Im, S.J., Kim, J.H., Kim, H.J., Kim, J.P. and Min, B.R. (2008), "Polyamide thin-film nanofiltration membranes containing TiO2 nanoparticles", *Desalination*, **219**(1-3), 48-56.
Lefevre, E., Bossa, N., Wiesner, M.R. and Gunsch C.K. (2016) "A review of the environmental implications of in situ remediation by nanoscale zero valent iron (nZVI): Behavior, transport and impacts on microbial communities", *Sci. Total Environ.*, **565**, 889-901.
Li, J., Xu, Z., Yang, H., Yu, L. and Liu, M. (2009), "Effect of TiO2 nanoparticles on the surface morphology and performance of microporous PES membrane", *Appl. Surf. Sci.*, **255**, 4725-4732.
Li, X.Q., Elliott, D.W. and Zhang, W.X. (2006), "Zero-valent iron nanoparticles for abatement of environmental pollutants: materials and engineering aspects", *Crit. Rev. Solid State Mater. Sci.*, **31**(4), 111-122.
Li, Z., Greden, K., Alvarez, P.J., Gregory, K.B. and Lowry, G.V. (2010), "Adsorbed polymer and NOM limits adhesion and toxicity of nanoscale zerovalent iron to E. coli", *Environ. Sci. Technol*., **44**(9), 3462-3467.
Liang, J., Du, N., Song, S. and Hou, W. (2015), "Magnetic demulsification of diluted crude oil-in-water nano emulsions using oleicacid-coated magnetite nanoparticles", *Colloid. Surf. A: Phys. Chem. Eng. Aspect.*, **466**, 197-202.
Liu, P.C., Hsieh, J.H., Li, C., Chang, Y.K. and Yang, C.C. (2009), "Dissolution of Cu nanoparticles and antibacterial behaviors of TaN-Cu nanocomposite thin films", *Thin Solid. Film.*, **517**, 4956-4960.
Ma, B., Yu, W., Jefferson, W.A., Liu, H. and Qu, J. (2015), "Modification of ultrafiltration membrane with nanoscale zerovalent iron layers for humic acid fouling reduction", *Water Res.*, **15**(71), 140-149.
Machado, S., Pinto, S.L., Grosso, J.P., Nouws, H.P.A., Albergaria, J.T. and Delerue-Matos, C. (2013), "Green production of zero-valent iron nanoparticles using tree leaf extracts", *Sci. Total Environ.*, **445**, 1-8.
Maity, D., Kale, S.N., Kaul-Ghanekar, R., Xue, J.M. and Ding, J. (2009), "Studies of magnetite nanoparticles synthesized by thermal decomposition of iron (III) acetylacetonate in tri (ethyleneglycol)", *J. Magnet. Magnet. Mater.*, **321**(19), 3093-3098.
Mansoori, G.A., Bastami, T.R, Ahmadpour, A. and Eshaghi, Z. (2008), "Environmental application of nanotechnology", *Ann. Rev. Nano Res.*, **2**, Chap. 2.
Mocé-Llivina, L., Jofre, J. and Muniesa, M., (2003), "Comparison of polyvinylidene fluoride and polyether sulfone membranes in filtering viral suspensions", *J. Virolog. Meth.*, **109**(1), 99-101.
Nikalje, A.P. (2015), "Nanotechnology and its applications in medicine", *Med. Chem.*, **5**(2), 81-89.
Özdemir, G., Limoncu, M.H. and Yapar, S. (2010), "The antibacterial effect of heavy metal and cetylpridinium-exchanged montmorillonites", *Appl. Clay Sci*., **48**, 319-323.
Pivin, J.C., Sendova-Vassileva, M., Lagarde, G., Singh, F. and Podhorodecki, A. (2006), "Optical activation of Eu3+ ions by Ag nanoparticles in ion exchanged silica-gel films", *J. Phys. D: Appl. Phys*., **39**, 2955-

2958.
Qiu, X., Fang, Z., Yan, X., Cheng, W. and Lin, K. (2013), "Chemical stability and toxicity of nanoscale zero-valent iron in the remediation of chromium contaminated watershed", *Chem. Eng. J.*, **220**, 61-66.
Rajabi, H., Ghaemi, N., Madaeni, S.S., Daraei, P., Astinchap, B., Zinadini, S. and Razavizadeh, S.H. (2015), "Nano-ZnO embedded mixed matrix polyethersulfone (PES) membrane: Influence of nano filler shape on characterization and fouling resistance", *Appl. Surf. Sci.*, **349**, 66-77.
Rehan, Z.A., Gzara, L., Khan, S.B., Alamry, K.A., El-Shahawi, M.S., Albeirutty, M.H., Figoli, A., Drioli, E. and Asiri, A.M. (2016), "Synthesis and characterization of silver nanoparticles-filled polyethersulfone membranes for antibacterial and anti-biofouling application", *Rec. Patent. Nanotech.*, **10**(2), 1-21.
Rosas, I., Collado, S., Gutiérrez, A. and Díaz, M. (2014), "Foulingmechanisms of *Pseudomonas putida* on PES microfiltrationmembranes", *J. Membrane Sci*., **465**, 27-33.
Rosenberger, I., Strauss, A., Dobiasch, S., Weis, C., Szanyi, S., Gil-Iceta, L., Alonso, E., GonzálezEsparza, M., Gómez-Vallejo, V., Szczupak, B., Plaza-García, S., Mirzaei, S., Israel, L.L., Bianchessi, S., Scanziani, E., Lellouche, J.P., Knoll, P., Werner, J., Felix, K., Grenacher, L., Rees, T., Kreuter, J. and Jiménez-González, M. (2015), "Targeted diagnostic magnetic nanoparticles formed ical imaging of pancreaticcancer", *J. Controll. Rel.*, **214**, 76-84.
Sciancalepore, C., Rosa, R., Barrera, G., Tiberto, P., Allia, P. and Bondioli, F. (2014), "Microwave-assisted non aqueous sol-gel synthesis of highly crystalline magnetite nanocrystals", *Mater. Chem. Phys.*, **148**(1), 117-124.
Shi, J., Yi, S., Long, C. and Li, A. (2015), "Effect of Fe loading quantity on reduction reactivity of nano zero-valent iron supported on chelating resin", *Front. Environ. Sci. Eng*., **9**(5), 840-849.
Sies, H. (1997), "Oxidative stress: oxidants and antioxidants", *Exp. Physiol*., **82**(2), 291-295.
Simeonidis, K., Kaprar, E., Samaras, T., Angelakeris, M., Pliatsikas, N., Vourlias, G., Mitrakas, M. and Andritsos, N. (2015), "Optimizing magnetic nanoparticles for drinking water technology: The case of Cr(VI)", *Sci. Total Environ.*, **535**, SI 61- 68.
Sumin, K. and Lim, H.B. (2015), "Chem iluminescence immunoassay using magnetic nanoparticles with targeted inhibition for the determination of ochratoxin A", *Talanta*, **140**, 183-188.
Sun, Y.P., Li, X.Q., Cao, J., Zhang, W.X. and Wang, H.P. (2006), "Characterization of zero-valentiron nanoparticles", *Adv. Colloid. Interf. Sci*., **120**, 47-56.
Suwal, S., Roblet, C., Amiot, J., Doyen, A., Beaulieu, L., Legault, J. and Bazinet, L. (2014), "Recovery of valuable peptides from marine protein hydrolysate by electrodialysis with ultrafiltration membrane: impact of ionic strength", *Food Res. Int.*, **65**, 407-415.
Taurozzi, J.S., Arul, H., Bosak, V.Z., Burban, A.F., Voice, T.C., Bruening, M.L. and Tarabara, V.V. (2008), "Effect of filler incorporation route on the properties of polysulfone silver nanocomposite membranes of different porosities", *J. Membr. Sci*., **325**, 58-68.
Teja, A.S. and Koh, P.Y. (2009), "Synthesis, properties, and applications of magnetic iron oxide nanoparticles", *Prog. Crystal Growth Character. Mater.*, **55**, 22-45.
Tina, L., Pouliot, P., Avti, P.K., Lesage, F. and Kakkar, A.K. (2013), "Superparamagnetic iron oxide based nanoprobes for imaging and theranostics", *Adv. Colloid Interf. Sci*., **199-200**, 95-113.
Toroghi, M., Raisi, A. and Aroujalian, A. (2014), "Preparation and characterization of polyethersulfone/silver nanocomposite ultrafiltration membrane for antibacterial applications", *Polym. Adv. Technol*., **25**, 711-722.
Vatanpour, V., Madaeni, S.S., Rajabi, L., Zinadini, S. and Derakhshan, A.A. (2012), "Boehmite nanoparticles as a new nanofiller for preparation of antifouling mixed matrix membranes", *J. Membrne Sci*., **401-402**, 132-143.
Wang, C.B. and Zhang, W.X. (1997), "Synthesizing nanoscale iron particles for rapid and completed echlorination of TCE and PCBs", *Environ. Sci. Technol*., **31**, 2154-2156.
Weiming, H., Jun, Y., Baolin, D. and Zhiqang, H. (2015), "Application of nano TiO2 modified hollow fiber membranes in algal membrane bioreactors for high-density algae cultivation and wastewater polishing", *Biores. Technol.*, **193**, 135-141.
Yan, W., Lien, H., Koel, B.E. and Zhang, W. (2013), "Iron nanoparticles for environmental clean-up: recent

developments and future outlook. Environ", *Sci. Proc. Impact.*, **15**(1), 63-77.
Yang, Y.X., Liu, M.L., Zhu, H., Chen, Y.R., Mu, G.J., Liu, X.N. and Jia, Y.Q. (2008), "Preparation, characterization, magnetic property, and mössbauer spectra of the *β*-FeOOH nanoparticles modified by nonionic surfactant", *J. Magnet. Magnet. Mater.*, **320**(21), L132-L136.
Yao, Y., Miao, S., Liu, S., Ma, L.P., Sun, H. and Wang, S. (2012), "Synthesis, characterization, and adsorption properties of magnetic Fe3O4 graphene nanocomposite", *Chem. Eng. J.*, **184**, 326-332.
Yu, L., Hao, G., Gu, J., Zhou, S., Zhang, N. and Jiang, W. (2015), "Fe_3O_4/PS magnetic nanoparticles: Synthesis, characterization and their application as sorbents of oil from wastewater", *J. Magnet. Magnet. Mater.*, **394**, 14-21.
Yu, R.F., Chen, H.W., Cheng, W.P., Lin, Y.J. and Huang, C.L. (2014), "Monitoring of ORP, pH and DO in heterogeneous Fenton oxidation using nZVI as a catalyst for the treatment of azo-dye textile wastewater", *J. Taiwan Inst. Chem. Eng.*, **45**(3), 947-954.
Yurtsever, A., Sahinkaya, E., Aktaş, Ö., Uçar, D., Çınar, Ö. and Wang, Z. (2015), "Performances of anaerobic and aerobic membrane bioreactors for the treatment of synthetic textile wastewater", *Biores. Technol.*, **192**, 564-573.
Zodrow, K., Brunet, L., Mahendra, S., Li, D., Zhang, A., Li, Q. and Alvarez, P.J. (2009), "Polysulfone ultrafiltration membranes impregnated with silver nanoparticles show improved biofouling resistance and virus removal", *Water Res.*, **43**(3), 715-723.

CC